Nucleic Acids Research, 2024, **52**, 11806–11821
https://doi.org/10.1093/nar/gkae792
Advance access publication date: 25 September 2024
Molecular and Structural Biology

A transcription-independent role for HIF-1α in modulating microprocessor assembly

Jie-Ning Li[1,2,3,4], Ming-Yang Wang[5,6], Jhen-Wei Ruan[1,2,4], Yu-Jhen Lyu[2,5], Yi-Hsiu Weng[1,2,4], Pownraj Brindangnanam[7], Mohane Selvaraj Coumar[7] and Pai-Sheng Chen[1,2,3,4,*]

[1]Institute of Basic Medical Sciences, College of Medicine, National Cheng Kung University, Tainan, Taiwan
[2]Department of Medical Laboratory Science and Biotechnology, College of Medicine, National Cheng Kung University, Tainan, Taiwan
[3]Breast Medical Center, National Cheng Kung University Hospital, Tainan, Taiwan
[4]Research Center for Medical Laboratory Biotechnology, National Cheng Kung University, Tainan, Taiwan
[5]Department of Surgery, National Taiwan University Hospital, Taipei, Taiwan
[6]Department of Surgical Oncology, National Taiwan University Cancer Center, Taipei, Taiwan
[7]Department of Bioinformatics, School of Life Sciences, Pondicherry University, Kalapet, Pondicherry 605014, India

[*]To whom correspondence should be addressed. Tel: +886 6 2353535; Fax: +886 6 2363956; Email: bio.benson@gmail.com; z10108021@ncku.edu.tw

Abstract

Microprocessor is an essential nuclear complex responsible for the initial RNase-mediated cleavage of primary miRNA, which is a tightly controlled maturation process that requires the proper assembly of Drosha and DGCR8. Unlike previously identified mechanisms directly targeting the enzymatic subunit Drosha, current knowledge about the biological ways of controlling miRNA nuclear maturation through DGCR8 is less addressed. In this study, we unveiled that the microprocessor assembly is governed by a master gene regulator HIF-1α irrespective of its canonical transcriptional activity. First, a widespread protein binding of HIF-1α with DGCR8 instead of Drosha was observed in response to biological stimulations. Similar protein interactions between their corresponding orthologues in model organisms were also observed. After dissecting the essential protein domains, we noticed that HIF-1α suppresses microprocessor assembly via binding to DGCR8. Furthermore, our results showed that HIF-1α hijacks monomeric DGCR8 thus reducing its dimer formation prior to microprocessor assembly, and consequently, the suppressed microprocessor formation and nuclear processing of primary miRNA were demonstrated. In conclusion, here we unveiled the mechanism of how microprocessor assembly is regulated by HIF-1α, which not only demonstrates a non-transcriptional function of nuclear HIF-1α but also provides new molecular insights into the regulation of microprocessor assembly through DGCR8.

Graphical abstract

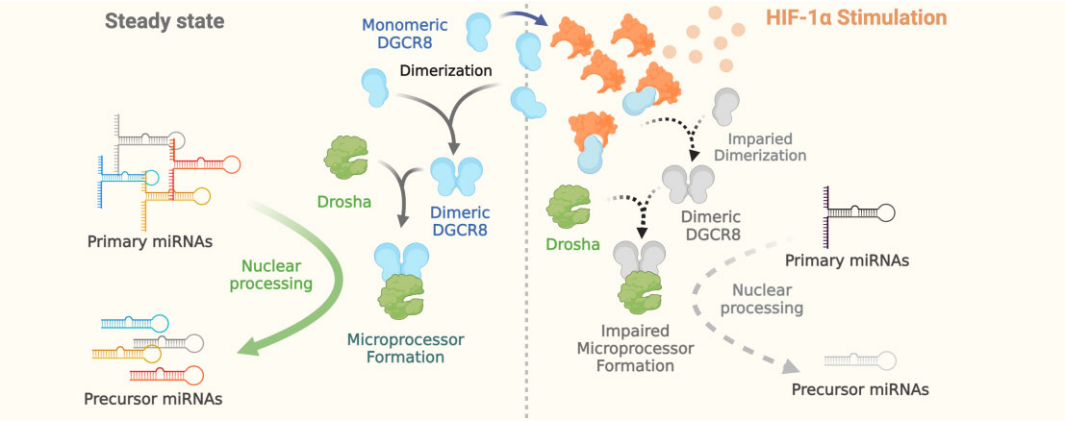

Introduction

MicroRNAs (miRNAs) are highly conserved small non-coding RNAs that post-transcriptionally regulate gene expression through sequence complementarity to 3′ untranslated region (3′ UTR) of target messenger RNA (mRNA), leading to translational inhibition or degradation of target mRNAs (1–4). MiRNA biogenesis is a multistep process relying on several factors to coordinate sequentially. First, the initial precursors are transcribed by RNA polymerase II (Pol II) as primary miRNAs (pri-miRNAs) with stem-loop and flanking

Received: January 5, 2024. **Revised:** August 22, 2024. **Editorial Decision:** August 27, 2024. **Accepted:** August 31, 2024

regions (5–7). In the nucleus, the microprocessor composed of RNase III enzyme Drosha and double-stranded RNA binding protein DGCR8 is responsible for the first step of RNase-dependent cleavage that cuts the flanking regions out from pri-miRNAs into single stem-loop precursor miRNAs (pre-miRNAs) (8,9). After being exported into the cytoplasm by Exportin 5, these pre-miRNAs are further cleaved by the second RNases III enzyme Dicer into 20–25 nucleotides long mature miRNAs. Finally, these mature miRNAs are loaded into miRNA-induced silencing complex (miRISC) composed by AGO2 and GW182/TRNC6A to execute their molecular function in post-transcriptional gene silencing (10,11).

The highly conserved enzymatic subunit Drosha of microprocessor was first identified in *D.melanogaster, C.elegans*, and eukaryotes by Filippov *et al.* (12), while its function in nuclear processing of miRNA was later discovered in 2003 by Lee *et al.* (9). Then, DGCR8 was identified as an essential component for miRNA processing functioning in the Drosha-associated protein complex called microprocessor thereafter (13–15). An intact microprocessor is composed of one Drosha and two DGCR8 proteins (16), while the dimerized DGCR8 binds with Drosha through its 23-amino acids long C-terminal tail region (CTT) and double-strand RNA-binding domains (dsRBDs) to enhance the loading of pri-miRNA. As the major nuclear processing complex for miRNA maturation, several regulatory mechanisms affecting microprocessor activity have been studied which mostly focused on gene regulation or protein interaction of Drosha in the past (1,17), but current knowledge on the biological control of DGCR8 is limited.

Hypoxia-inducible factor 1-alpha (HIF-1α) is a master transcriptional regulator stimulated under different microenvironmental circumstances including hypoxic (low oxygen concentration) and non-hypoxic factors (growth factors, reactive oxygen species, and nutrient depletion) (18–25). Our previous study has indicated that cytoplasmic HIF-1α suppresses miRNA biogenesis through promoting autophagic proteolysis of Dicer (26). However, as a well-known transcription factor enriched in cell nuclei, the link between HIF-1α and nuclear processing of miRNAs remains unclear. In this study, we unveiled that the nuclear processing of miRNA is controlled by HIF-1α independent of its well-known transcriptional activity, in which HIF-1α prevents DGCR8 dimerization and leads to repressed microprocessor assembly as well as the nuclear maturation of miRNA precursors.

Materials and methods

Cell culture

Human embryonic kidney cell line (HEK293T), lung cancer (A549), cervical cancer (HeLa), colorectal cancer (HCT116), hepatocellular cancer (Huh7) and breast cancer cells (MDA-MB-231) were cultured in Dulbecco's modified Eagle's medium/nutrient mixture F-12 (DMEM/F12) medium supplement with 10% fetal bovine serum (FBS, Corning®) and 1% penicillin/streptomycin antibiotics. Breast cancer cells (MCF-7) were cultured in low-glucose Dulbecco's modified Eagle's medium (DMEM). All human cancer cell lines were grown at 37°C in the 5% CO_2 humidified incubator.

Protein extraction

Cells were rinsed by PBS twice and harvested using RIPA buffer (50 mM Tris base, 150 mM NaCl, 10% NP-40, 0.5% Na-deoxycholate, 1 mM EDTA and 0.1% SDS). After sonication, total cell lysate was centrifuged for 14 000 rpm, 30 min and the supernatant was collected and quantified using Bradford assay by detecting absorbance at 595 nm.

Immunoprecipitation

Cells were rinsed by PBS twice and lysed by NETN lysis buffer (150 mM NaCl, 20 Mm Tris–HCl; pH 8.0, 0.5% NP-40, 1 mM EDTA) containing 1× complete protease inhibitors (Pierce™, A32965). Cell lysates were sonicated and centrifuged at 14 000 rpm for 30 min at 4°C to remove cell debris. For *D. melanogaster* and *C. elegans* protein extraction, whole flies were homogenized first in NETN lysis buffer and sonicated; worms were collected in NETN lysis buffer and followed by sonication. Sonicated lysates were centrifuged at 14 000 rpm for 30 min at 4°C and collected supernatants. After quantification, lysates were pre-cleaned with Pierce™ Protein A Plus Agarose for an hour and rotated at 4°C. Lysates were centrifuged at 2500 rpm for 5 min to remove beads and supernatant were collected and incubated with the specific antibody at 4°C overnight (Anti-DGCR8: Bethyl, A302-468A; Anti-Drosha: Santa Cruz, Sc-33778; Anti- HIF-1α: Genetex Inc, GTX127309; Anti-Flag: Sigma, F3165). Next day, lysates were incubated with agarose beads for an hour at 4°C and washed the beads by NETN buffer for 2 times, 5 min at 2500 rpm. The immunoprecipitated samples were further applied to western blot analysis.

Western blot

Denatured protein lysate was loaded and fractionated by SDS-PAGE. Proteins in SDS-PAGE were transferred onto PVDF membranes according to the manufacturer's protocols (Bio-Rad, Hercules, CA, USA). PVDF (GE Healthcare) was blocked with 5% skimmed milk for an hour at room temperature and washed with TBST. Membranes were incubated with specific primary antibodies at 4°C for overnight (Anti-DGCR8: Bethyl, A302-468A; Anti-Drosha: Cell Signaling, #3364; Anti- HIF-1α: Novus Biologicals, NB100-449; Anti-Flag: Sigma, F3165; Anti-V5: Genetex Inc, GTX117997). After washed by TBST for 3 times, 10 min per wash, the membranes were incubated with secondary antibodies (Croyez Bioscience, Taiwan) for an hour at room temperature. Protein expressions were detected by ECL system according to the manufacturer's protocols. ECL (Enhanced Chemiluminescent) was purchased from PerkinElmer (Waltham, MA, USA).

Total RNA extraction

Total RNA was extracted using TRIzol (Invitrogen) according to the manufacturer's protocol. In brief, lysed cells in TRIzol reagent were incubated with chloroform and homogenized samples were centrifuged at 14 000 rpm for 30 min at 4°C. The clear aqueous middle layer was isolated, and RNA was precipitated by incubating with isopropanol at −80°C for 1–2 h. Samples were centrifuged at 14 000 rpm for 30 min, and the supernatant was discarded. The pellets were washed with 75% ethanol and centrifuged again. Pellets were dissolved and preserved in nuclease-free water at −80°C. Total RNA concentrations were determined by spectrophotometer (NanoDrop Lite Microlitre Spectrophotometer).

Reverse transcription

Reverse transcription (RT) was performed immediately after RNA quality control assessment and the same amount of RNA was used in each sample. Reverse transcription was performed using the M-MLV Reverse Transcriptase (PROMEGA, Cat. #M1701) according to the manufacturer's protocol. The reaction mixture contained 200 ng of template RNA, 1 μl 100 μM random hexamer, and 2 μl 10 mM dNTP mix with nuclease-free water adjusted to 12 μl and performed pre-RT process incubating at 65°C for 5 min. Mix of 4 μl 5X reaction buffer, 0.6 μl M-MLV Reverse Transcriptase and 0.4 μl RNase inhibitor (RNasin, Cat. #N2515) was added, the volume was brought to 20 μl with nuclease-free water, and the reactions were incubated at 25°C for 5 min, followed by 37°C for 60 min. Finally, the reactions were terminated at 70°C for 5 min. cDNAs were preserved at −20°C and further applied to quantitated real-time PCR. To perform the reverse transcription of pre-miRNAs, RNAs shorter than 200 nucleotides were further enriched by using mirVana™ miRNA Isolation Kit (Invitroge™, AM1560) for pre-miRNAs detection. Pre-RT process incubating RNAs with pre-miRNA specific primer at 85°C for 5 min was performed to unravel the secondary structure and reverse transcription was performed by the protocol mentioned above.

Quantitated real-time PCR

Quantitated real-time PCR was performed using qPCRBIO SyGreen Mix according to the manufacturer's protocols by Applied Biosystem Step One Real-time PCR system (Applied Biosystems, CA, USA). Specific primers for targets (Supplementary Table S1) were designed with an amplicon range from 50–200 nucleotides. Mixture consisted of SYBR GREEN Master Mix, forward and reverse primers, nuclease-free water and cDNA template. The real-time PCR program was carried out according to the manufacturer's protocol, which included 95°C for 10 min to activate the polymerase, 40 cycles of 95°C for 15 s and 60°C for 1 min followed by melt-curve analysis. All the qPCR protocols followed MIQE guidelines (27).

Unprocessed pri-miRNAs and pre-miRNAs detection

Primers for detecting unprocessed pri-miRNAs were based on the principle that primers were complemented to the flanking region and stem region across through the processed site of pri-miRNAs (Supplementary Table S1). The primers detecting unprocessed pri-miRNAs are able to distinguish the pri-miRNAs from pre-miRNAs which have the same sequences in the stem loop region. To determine the pre-miRNAs produced by microprocessor, cell nuclei were isolated by NE-PERTM Nuclear and Cytoplasmic Extraction Reagents (Thermo Scientifi™, Cat. 78 833), RNAs shorter than 200 nucleotides were further enriched by using mirVana™ miRNA Isolation Kit (Invitroge™, AM1560) for nuclear pre-miRNAs detection. All the qPCR detection protocols followed MIQE guidelines (Supplementary Table S1) (27).

In vitro transcription and *in vitro* processing assay

In vitro transcription was performed using T7 RiboMAX™ Express Large Scale RNA Production System (Promega, Cat. #P1320) according to the manufacturer's protocol. These well-structured, unprocessed pri-miRNAs produced from *in vitro* transcription were collected as the substrates for *in vitro* processing assay. Cell extracts were collected and incubated with *in vitro* synthesized pri-miRNAs (100 ng) in *in vitro* processing buffer (50 mM Tris, 2 mM DTT, 6 mM $MgCl_2$) at 37°C for 30 min (9,28,29). RNA was extracted after *in vitro* processing assay and performed reverse transcription and quantitated real-time PCR for unprocessed pri-miRNAs and pre-miRNAs detection.

Luciferase activity assay

Renilla and firefly reporter activity were measured using The Dual-Luciferase® Reporter (DLRTM) Assay System according to the manufacturer's protocols. Briefly, the firefly luciferase activity was measured first by Luciferase Assay Reagent II (LAR II) and next, the reaction was quenched, followed by adding Stop & Glo® Reagent for detecting renilla luminescence in the same sample.

Constructs

Microprocessor reporter plasmids were gift from Dr Richard I. Gregory (30). The portions of pri-miR-125b and pri-miR-205 were inserted into 3′ UTR of renilla luciferase gene in psiCHECK2 plasmid (30). HIF-1α gene was constructed into pcDNA3.1 and a panel of HIF-1α truncated plasmids were cloned into pcDNA3.1 by Dr Chih-Chen Hong (26). DGCR8 gene was constructed into pcDNA3.1 and DGCR8 with truncated double strand RNA binding domain 1 (dsRBD1), Drosha-binding element and uncharacterized region from 685 to 773 were cloned into pcDNA3.1 by Dr Chih-Chen Hong. Flag-DGCR8 were kindly provided by Dr V. Narry Kim (31). PcDNA3-V5-DGCR8 was acquired from Addgene (#51 383) (14). Constructs expressing wild-type and point mutations of DGCR8 (W329A and W329H) were kindly provided from Dr Feng Guo (32). BiFC platform plasmids (VC155-HIF-1α and VN173-DGCR8) were cloned by the National RNAi Core Facility at Academia Sinica in Taiwan. PcDNA3-pri-let-7a (#51 377), pcDNA3-pri-let-7b (#51 378), pcDNA3-pri-let-7d (#51 379), pcDNA3-pri-let-7e (#51 380), pcDNA3-pri-let-7g (#51 381), pcDNA3-pri-miR-16–1 (#51 382), pcDNA3-miR-29b-1∼29a (#51 376) and pcDNA3.2/V5 hsa-mir-205 (#26 312) for *in vitro* transcription were acquired from Addgene (33,34).

Genes manipulation: transfection and shRNAs interference assay

Transfection was performed using HyFect™ DNA transfection reagent according to the manufacturer's protocol (Leadgene Biomedical, Taiwan). The plasmids were incubated with transfection reagent in serum-free medium for 20 min and added into cells. ShRNAs were carried by lentivirus produced by HEK293T. HEK293T cells were seeded and transfected with packaging plasmid (pCMV-ΔR8.91 containing gag, pol and rev genes), envelope plasmid (pMD.G, VSV-G expressing plasmid) and pLKO.1-shRNA vector with shRNAs complementary to target protein. Virus-containing medium was collected after 24 and 48 h. Cells were infected with lentivirus carrying shRNA and polybrene was added to enhance infectious efficiency. Protein lysate was harvested and check the target protein expression by western blot.

Growth factor treatment and hypoxic condition

MDA-MB-231 cells were seeded and starvation for 24 h and treated with EGF (40 ng/ml) or IGF (100 ng/ml) for 24 h. MCF-7 or MDA-MB-231 cells were incubated in the hypoxia chamber (1% O_2) for 6 h.

In situ proximity ligation assay (PLA)

In situ PLA was performed according to the manufacturer's instructions (Sigma-Aldrich). Multiple cancer cell lines were seeded onto cover slides in a 12-well plate. Tissue microarrays were dried before use in an oven at 60°C, one hour and immersed slides in water. The slides were fixed with 3.7% formaldehyde for 10 min, permeabilized by 0.01% triton-X-100 for 10 min, blocking with 2% bovine serum albumin (BSA) for 30 min at room temperature. Two primary antibodies of interested protein from different host were applied to slides or tissue microarray at 4°C for overnight (Anti-DGCR8: Abnova, H00054487-B01P; Anti- HIF-1α: Novus Biologicals, NB100-449; Anti-Drosha: Santa Cruz, Sc-33778). One primary antibody (Anti-DGCR8: Abnova, H00054487-B01P) was used as a negative control. The samples were washed by buffer A for 2 times, 5 min and secondary antibodies conjugated with oligonucleotides were added and incubated at 37°C for 1 hour. Next, performed the ligation step at 37°C for 30 min and amplification process was performed at 37°C for 100 min in the dark. Then, washed with buffer b for 10 min and mounted the slides and tissue microarrays. During the whole process, slides and tissue microarrays were kept in a humidified chamber.

Tissue microarray

Tissue microarray CBA4 (SUPER BIO CHIPS) and BRC1021 (US Biomax lnc.) breast cancer tissues were applied to PLA for interaction between HIF-1α/DGCR8, DGCR8/Drosha, DGCR8/RRP6 and HIF-1α protein expression. Tissue microarrays were used according to approved IRB protocols from NCKU Hospital (IRB No. A-ER-105–491, A-ER-106-483).

Human subjects

We analyzed samples of breast cancer tissues from individual patients. Specimens were collected from National Cheng Kung university hospital (Tainan, Taiwan). Frozen breast cancer tissues were used according to approved IRB protocols from NCKU Hospital (IRB No. A-ER-103–131, A-ER-105–491, A-ER-106–483).

Model organism information

Caenorhabditis elegans strains were maintained and grown on nematode growth media (NGM) and fed with *E. coli* OP50 at 20°C. Alkaline hypochlorite solution was used for synchronization of well-fed adult animals and the synchronized populations were grown on *E. coli* OP50 to the day-1 adult stage for 3 days at 20°C. All strains in this study were provided by Caenorhabditis Genetics Center (CGC), including N2-Bristol, *hif-1 (ia4), and ials34 [Phif-1::hif-1(P621G)::myc]*. Drosophila melanogaster was maintained on standard food at 25°C on a normal circadian cycle (12:12 light dark cycle). Gal4 drivers were crossed with UAS-simaRNAi (P[TRiP.HMS00833]) lines.

Quantification and statistical analysis

All of data were analyzed by using Prism 9 (GraphPad, La Jolla, CA) and the results are presented as mean ± SEM. at least three independent experiments. Unpaired two-tailed *t*-test was used for two individual groups. For multigroup analysis, one-way ANOVA with Tukey's multiple comparisons test was used.

Results

HIF-1α non-transcriptionally suppresses nuclear processing of pri-miRNAs

MicroRNA (miRNA) biogenesis is a two-step process sequentially conducted from the nucleus to cytoplasm (17). Our previous study has shown that hypoxia inducible factor-1α (HIF-1α) suppresses Dicer-mediated miRNA maturation in the cytoplasm (26). As a well-studied transcription factor which mainly functions in the nucleus (19), we were curious about the effect of HIF-1α on nuclear miRNA processing which is carried out by the so-called Microprocessor complex composed of Drosha and DGCR8 for cleaving primary (pri-miRNA) into precursor (pre-miRNA) miRNA (17). To determine the processing efficiency of microprocessor, we utilized a reporter system established by Mori *et al.* harboring pri-miRNA sequences (pri-miR-125b and pri- miR-205) as the microprocessor substrates in the 3′ UTR of the Renilla luciferase gene (30); thus, the microprocessor-mediated cleavage resulted in destabilization of renilla luciferase mRNA as well as the luminescence signal, which as a denominator reflects to increased microprocessor activity. We first utilized this reporter assay to investigate the effect of HIF-1α on microprocessor function and observed that in HEK293T cells with ectopic HIF-1α expression, the microprocessor activity was significantly decreased (Figure 1A). There are several known possibilities which may modulate microprocessor activity, including the transcription regulation of *DROSHA* gene, the post-translational regulation of Drosha protein stability, and the physical interaction of Drosha with accessory factors (1,2,17). To investigate the mechanism of microprocessor suppression, protein levels of Drosha and DGCR8 were determined to investigate whether the expression of these microprocessor components is affected by HIF-1α. However, the protein expression of both components was not regulated by HIF-1α (Figure 1B, Supplementary Figure S1). As HIF-1α is a well-documented transcription factor, we further destroyed the DNA-binding ability of HIF-1α by truncating the basic helix-loop-helix DNA-binding motif (HIF-1$\alpha^{\Delta HLH}$) to study if the transcriptional activity of HIF-1α is essential for microprocessor regulation. Pyruvate dehydrogenase kinase 1 (PDK1), the known transcriptional downstream of HIF-1α (35) was confirmed to be upregulated by wild-type but not truncated HIF-1α (Figure 1C). Unchanged mRNA level of Drosha and DGCR8 were observed in wild-type and HLH-truncated HIF-1α (Figure 1D) and the HIF-1α-modulated microprocessor function was further investigated by the detection of either pri- (Figure 1E) or pre- (Figure 1F) miRNAs. Unexpectedly, HIF-1$\alpha^{\Delta HLH}$ still exhibited suppressive effects on nuclear pri- miRNA processing similar to that caused by wild-type HIF-1α, as our results consistently showed the accumulation of unprocessed substrates (pri-miR-125b/pri-miR-205) and reduction of cleaved products (pre-miR-125b/pre-miR-205) both in wild-type and HLH-truncated HIF-1α

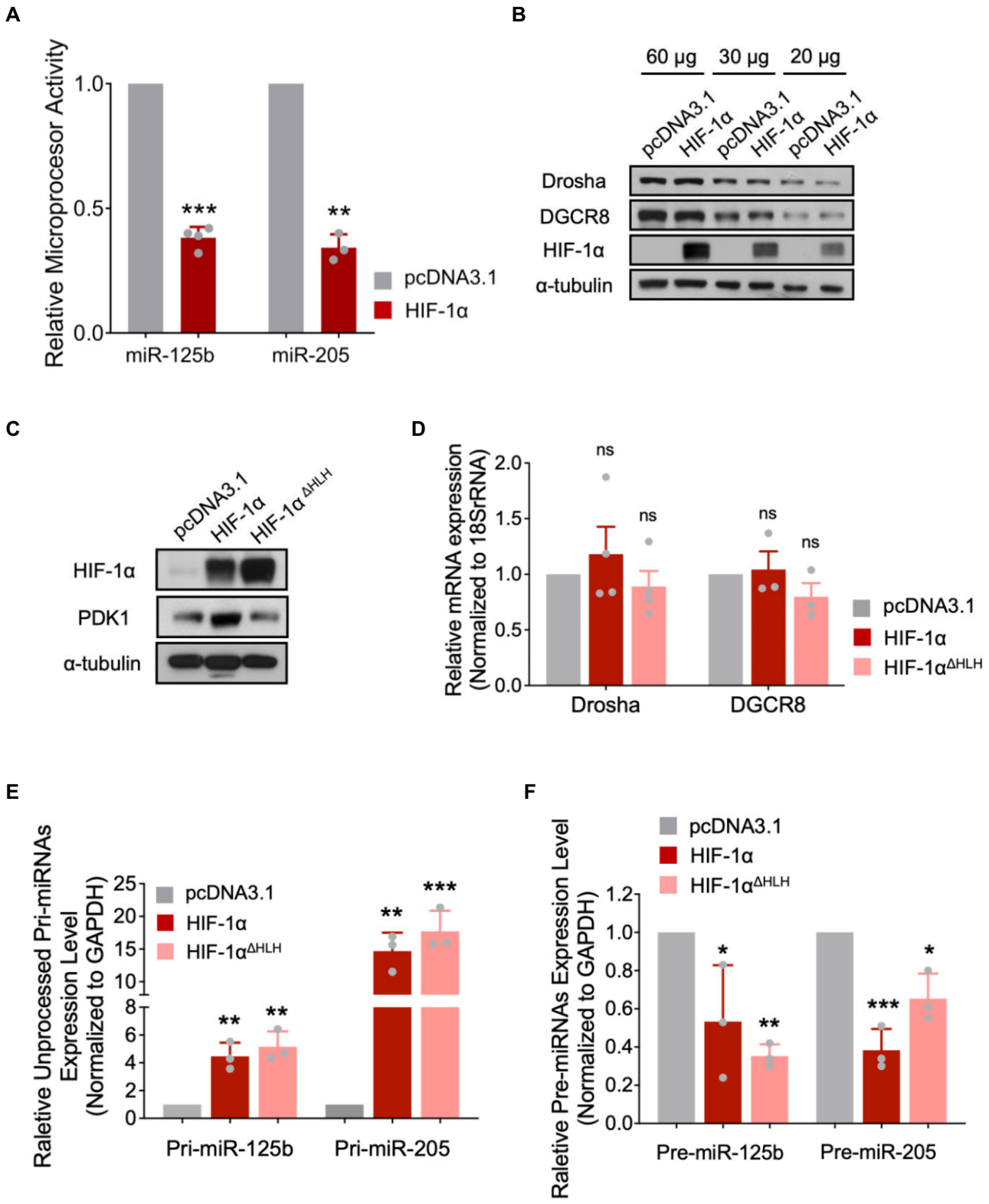

Figure 1. HIF-1α non-transcriptionally suppresses nuclear processing of pri-miRNAs. (**A**) Microprocessor activity was determined by luciferase reporter assay using HEK293T cells with ectopic HIF-1α expression. (**B**) Protein expression of Drosha, DGCR8 and HIF-1α in HEK293T cells with ectopic HIF-1α expression. (**C**) Validation of wild-type and HLH-truncated HIF-1α and PDK1 expression in HEK293T cells. (**D**) Messenger RNA expression of Drosha and DGCR8 in HEK293T cells with ectopic wild-type and HLH-truncated HIF-1α expression. (E-F) Expression of miRNAs precursors controlled by HIF-1α. Expression of pri- (**E**) and pre- (**F**) miRNAs of miR-125b and miR-205 in HEK293T cells with HIF-1α or HIF-1$\alpha^{\Delta HLH}$ expression. Data were represented as mean ± SEM ($n \geq 3$) with individual data point shown. $^{*}P < 0.05$, $^{**}P < 0.01$, $^{***}P < 0.001$.

expressing cells (Figure 1E, F). These results collectively suggested that HIF-1α suppresses miRNA nuclear processing in a transcription-independent manner.

Protein interaction of HIF-1α with DGCR8

Although it is possible that regulation on microprocessor expression directly affects microprocessor activity (1), we did not observe any significant change of either Drosha or DGCR8 protein expression regulated by HIF-1α (Figure 1B, D and Supplementary Figure S1), leading us to investigate the possibility of physical protein interaction between HIF-1α and microprocessor components. Interestingly, our immunoprecipitation assays showed that HIF-1α interacts with DGCR8 but not Drosha in HEK293T, MDA-MB-231 and MCF-7 cells (Figure 2A). A widespread HIF-1α/DGCR8 binding among different types of human cancer cell lines was also observed by immunoprecipitation and *in situ* PLA (Figure 2B, C), suggesting that this complex is widely present and not restricted to specific cell types. The presence of RNA could be a determining factor for protein–protein interaction, especially after the initiation step of microprocessor formation. Therefore, we performed RNase A treatment to investigate whether the endogenous binding of HIF-1α with DGCR8 is RNA-mediated or not. Our result showed that HIF-1α still interacts with DGCR8 in the presence of RNase A treatment, suggesting that this interaction is RNA-independent (Figure 2D). In addition to pull-down and PLA assays, we established the Bimolecular Fluorescence Complementation (BiFC) platform which is a powerful technique that allows the determination of direct protein interaction under a native biological system, as direct protein binding enables two independent fragments to reassemble into a functional fluorescent protein and emit a fluorescent signal (26,36–38). To confirm the interaction between HIF-1α and DGCR8 by BiFC assay, we designed two chimeric proteins, VC155-HIF-1α and VN173-DGCR8 by respectively constructing C-terminal of Venus protein to HIF-1α and N-terminal of Venus protein to DGCR8 (Figure 2E), and our results indicated a significant reconstitution of Venus fluorescence signal in cells expressing half of Venus-fused HIF-1α and DGCR8 (Figure 2E).

To elucidate the interaction of HIF-1α with DGCR8, we respectively performed genetic approaches including ectopic expression and knockdown of HIF-1α for binding assay, and found that HIF-1α/DGCR8 binding is greatly induced in HIF-1α-overexpressing cells (Figure 3A, left), while HIF-1α/DGCR8 interaction was also diminished in cells with HIF-1α knockdown (Figure 3A, right). In addition to genetic manipulations, biological stimulations such as hypoxia and growth factor stimulations including IGF and EGF were used to induce HIF-1α since these pathophysiological circumstances are HIF-1α-inducing biological factors (18,26). Consistently, our results indicated that the HIF-1α/DGCR8 binding is significantly accumulated in human cells with the treatment of CoCl2-stabilized HIF-1α (Figure 3B) as well as being exposed to hypoxia or stimulated by IGF and EGF (Figure 3C). Moreover, the interaction of HIF-1α with DGCR8 was observed in human breast (Figure 3D) and colon (Figure 3E) cancer tissues, suggesting that this complex is widely present in the human body. Altogether, these results demonstrated the suppressive role of HIF-1α in modulating microprocessor processing activity, and its selective binding to DGCR8 but not Drosha.

Identification of functional domains essential for reciprocal protein interaction

To investigate the structural characteristics of HIF-1α/DGCR8 binding, HIF-1α with individually truncated functional domain (Figure 4A) (26) were used for identifying protein region for interaction, and our results revealed that either oxygen-dependent degradation domain (ODD)- or inhibitory domain (ID)- truncated HIF-1α weakens its DGCR8 binding ability (Figure 4B, lanes 5–6). Noteworthy, the region from ODD to ID domain of HIF-1α proteins was predicted as intrinsically disordered regions (IDR) which are possible for protein-protein interaction (39), and similar structure was observed across human, mice, drosophila and nematode worms, even though their amino acid are poorly conserved (Figure 4C, ODD domain showed as blue and ID domain showed as yellow). Furthermore, HIF-1α and DGCR8 interacting residues were predicted using three computational simulation models built by ZDOCK, PatchDock, and HADDOCK (40,41). In combination with the known DGCR8/Drosha complex structure in RCSB PDB (PDB ID: 6V5B) and interacting residues in PDBsum (42), we found several DGCR8 residues simultaneously appeared in both DGCR8/HIF-1α and DGCR8/Drosha interface, while these HIF-1α-binding residues were mostly located in the C-terminal region (511–750) of DGCR8 (Figure 4D, upper panel). Therefore, we designed several DGCR8 constructs with individual truncations of known C-terminal functional domains including the double strand RNA binding domain 1 (dsRBD1), Drosha-binding element and an uncharacterized region from 685 to 773. (Figure 4D, bottom panel). The results turned out that truncation forms of either one of these regions disable the interaction between DGCR8 and HIF-1α (Figure 4E). More importantly, the regions essential for HIF-1α binding formed a conserved C-terminal 'helical arch' structure (Figure 4F, showed as blue) with 50–90% amino acid similarities (Figure 4G) among different model organisms, leading us to determine the existence of HIF-1α/DGCR8 complex in flies or worms. Consistently, bindings of HIF-1α with DGCR8 was also observed in both *Caenorhabditis elegans* (Figure 4H, DRSH-1, the human Drosha ortholog; PASH-1, the human DGCR8 ortholog; HIF-1, the human HIF-1α ortholog in *C.elegans*) and *Drosophila melanogaster* (Figure 4I, Pasha, the human DGCR8 ortholog; Sima, the human HIF-1α ortholog in *Drosophila melanogaster*), showing that protein interaction between the orthologs of HIF-1α and DGCR8 is preserved during evolution.

HIF-1α hijacks monomeric DGCR8 to suppress microprocessor formation

The precise molecular anatomy of microprocessor has been dissected which is composed of two DGCR8 and one Drosha (16). Sequentially, the dimerized DGCR8 is formed first and then complexes with Drosha as an intact functional microprocessor (Figure 5A) (16). In consideration of the results that the Drosha-binding element of DGCR8 is required for HIF-1α binding (Figure 4E), we further hypothesized a possibility of HIF-1α in regulating the microprocessor assembly (Figure 5B). Indeed, reduced Drosha/DGCR8 complex level was observed when ectopically expressing (Figure 5C, D) and stabilizing HIF-1α (Figure 5E), while knockdown of HIF-1α by three different specific shRNAs consistently enhanced the complex formation (Figure 5F, G). These effects

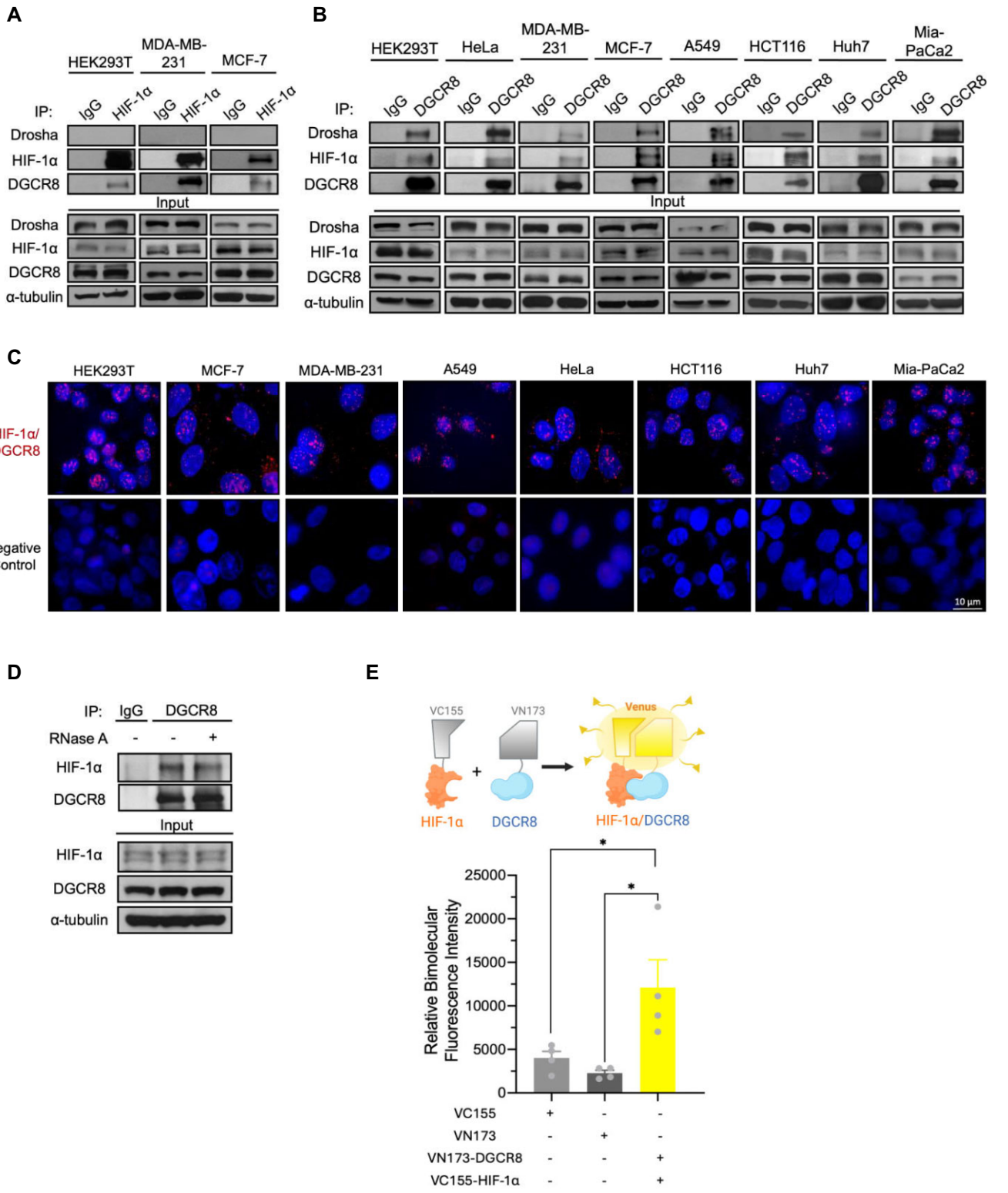

Figure 2. Interaction between HIF-1α and DGCR8. (A, B) Reciprocal assays for HIF-1α/DGCR8 binding. Interaction between HIF-1α and DGCR8 was determined by immunoprecipitation of endogenous HIF-1α (**A**), DGCR8 (**B**) in multiple cancer cell lines. (**C**) Visualization of HIF-1α/DGCR8 binding by *in situ* PLA in multiple cancer cell lines. (**D**) RNA dependency of the interaction between HIF-1α and DGCR8. Lysate was incubated with or without RNase A (200 μg/ml) for 30 min at 37°C, and immunoprecipitation of DGCR8 using anti-DGCR8 antibody was performed to detect endogenous binding between HIF-1α and DGCR8 in HEK293T cells. (**E**) Schematic representation of BiFC assay for the interaction between VC155-fused HIF-1α and VN173-fused DGCR8 (top). HEK293T cells were transfected with VC155-fused HIF-1α, VN173-fused DGCR8, or corresponding vector, and lysates were collected for Venus fluorescence signal detection. Data were represented as mean ± SEM ($n \geq 3$) with individual data point shown. *$P < 0.05$.

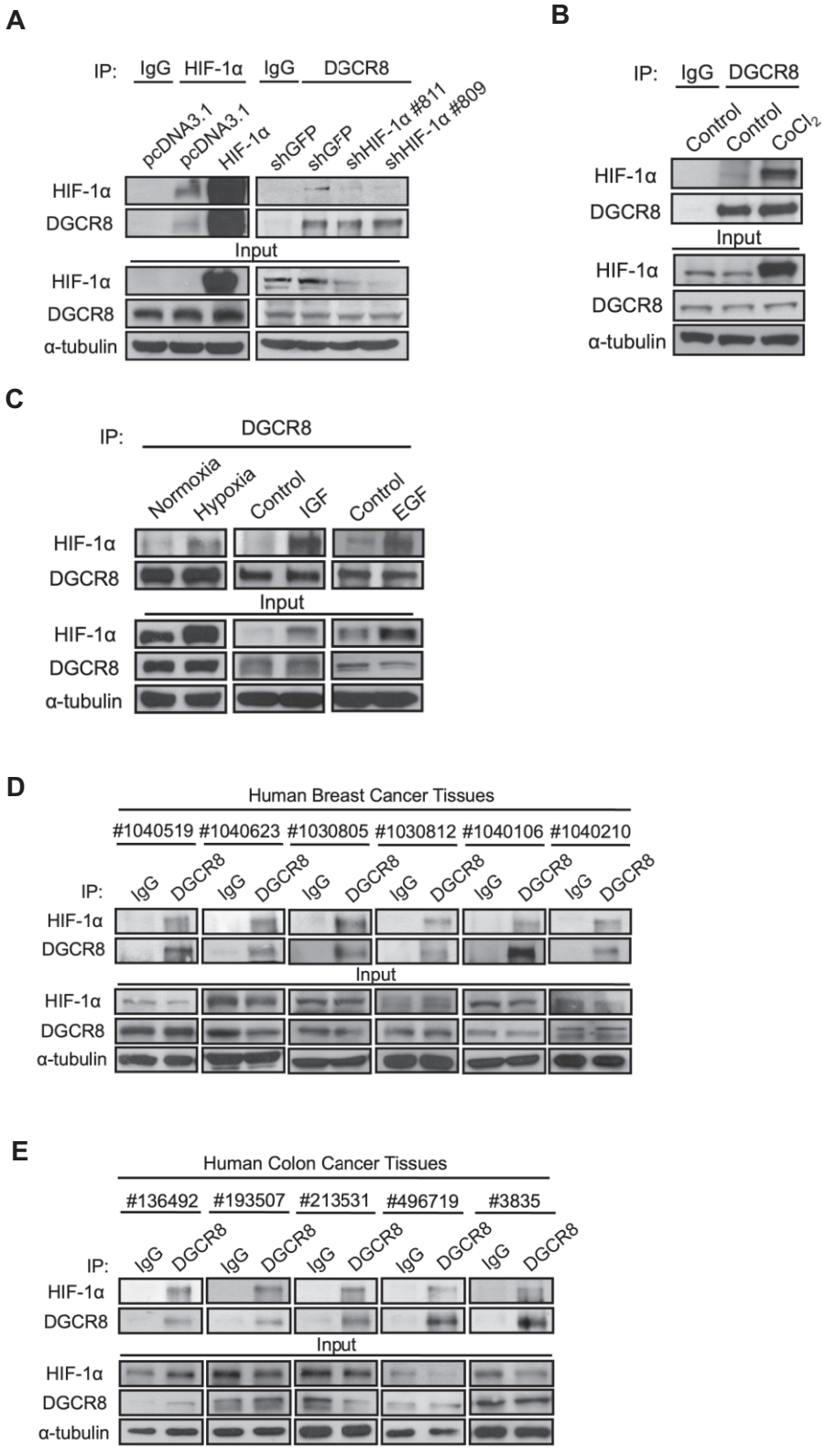

Figure 3. HIF-1α protein interacts with DGCR8 in response to biological stimulations and in human cancer tissues. (A–C) Interaction of HIF-1α/DGCR8 under genetic manipulations and biological stimulations. Genetically manipulated (**A**), chemically stabilized (**B**), and biologically stimulated (**C**) HIF-1α cells were applied to immunoprecipitation for determining the binding of HIF-1α/DGCR8. MDA- MB-231 cells were incubated under hypoxia (1% O_2) for 6 h or IGF (100 ng/ml)/EGF (40 ng/ml) treatment for 24 h. Binding of HIF-1α with DGCR8 in human breast (**D**) and human colon (**E**) cancer tissues.

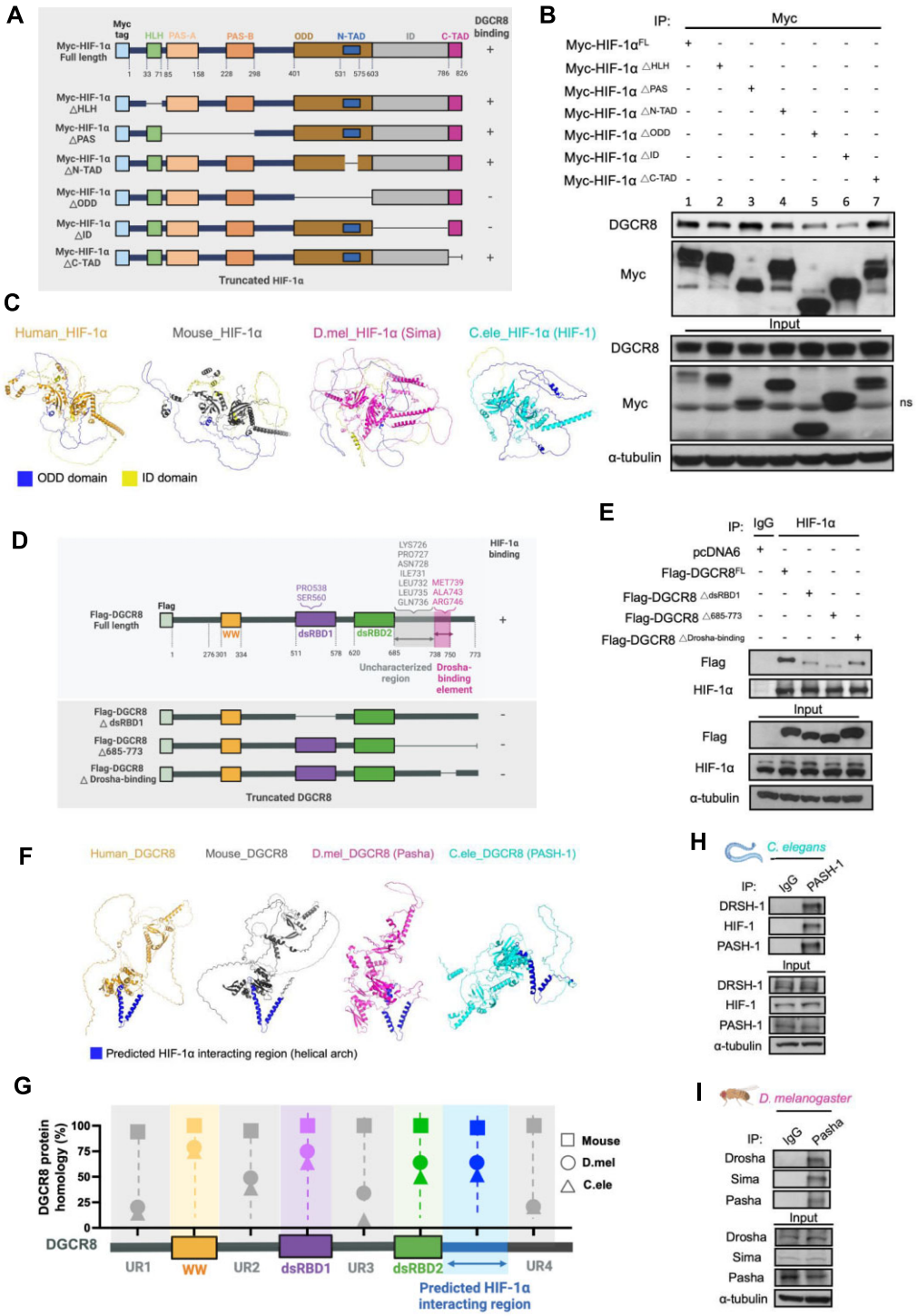

Figure 4. Identification of functional domain of HIF-1α and DGCR8 for reciprocal interaction. (**A**) Schematic representation of individual HIF-1α truncations. (**B**) Interactions of DGCR8 with truncated HIF-1α in HEK293T cells expressing indicated HIF-1α truncations were determined. (**C**) Protein structures of HIF-1α orthologs from human (UniProtKB: Q16665), mouse (UniProtKB: Q61221), *D.mel* (UniProtKB: Q24167) and *C.ele* (UniProtKB: G5EGD2) were predicted using AlphaFold (58) and recolored by PyMol (The PyMOL Molecular Graphics System, Version 2.0 Schrödinger, LLC). ODD and ID domains were respectively shown in blue and yellow. (**D**) HIF- 1α-interacting residues of DGCR8 were indicated in upper panel. Design of truncated DGCR8 constructs in bottom panel. (**E**) Interaction of HIF-1α with truncated DGCR8 in HEK293T cells expressing indicated DGCR8 truncations were determined. (**F**) Protein structure of DGCR8 orthologs from human (UniProtKB: Q8WYQ5), mouse (UniProtKB: Q9EQM6), *D.mel* (UniProtKB: Q9V9V7) and *C.ele* (UniProtKB: U4PRH5) were predicted using AlphaFold and recolored by PyMol. Predicted HIF-1α interacting region with a conserved helical arch structure was shown in blue. (**G**) DGCR8 protein homology percentage was aligned by COBALT using positive match as index by setting human as the reference sequence. Indicated regions of DGCR8 were independently analyzed for their evolutional homology in amino acid sequence. UR: uncharacteristic region. Positive match: considered as conservative substitution. (H-I) HIF- 1α/DGCR8 binding in model organisms. Interaction between HIF-1α and DGCR8 was determined by immunoprecipitation of endogenous DGCR8 in *Caenorhabditis elegans* (*C. elegans*, **H**) and *Drosophila melanogaster* (*D. melanogaster*, **I**). DRSH-1, HIF-1, PASH-1 are respectively human Drosha, HIF-1α, DGCR8 orthologs in *C.elegans*; Sima and Pasha are respectively human HIF-1α and DGCR8 orthologs in *D. melanogaster*.

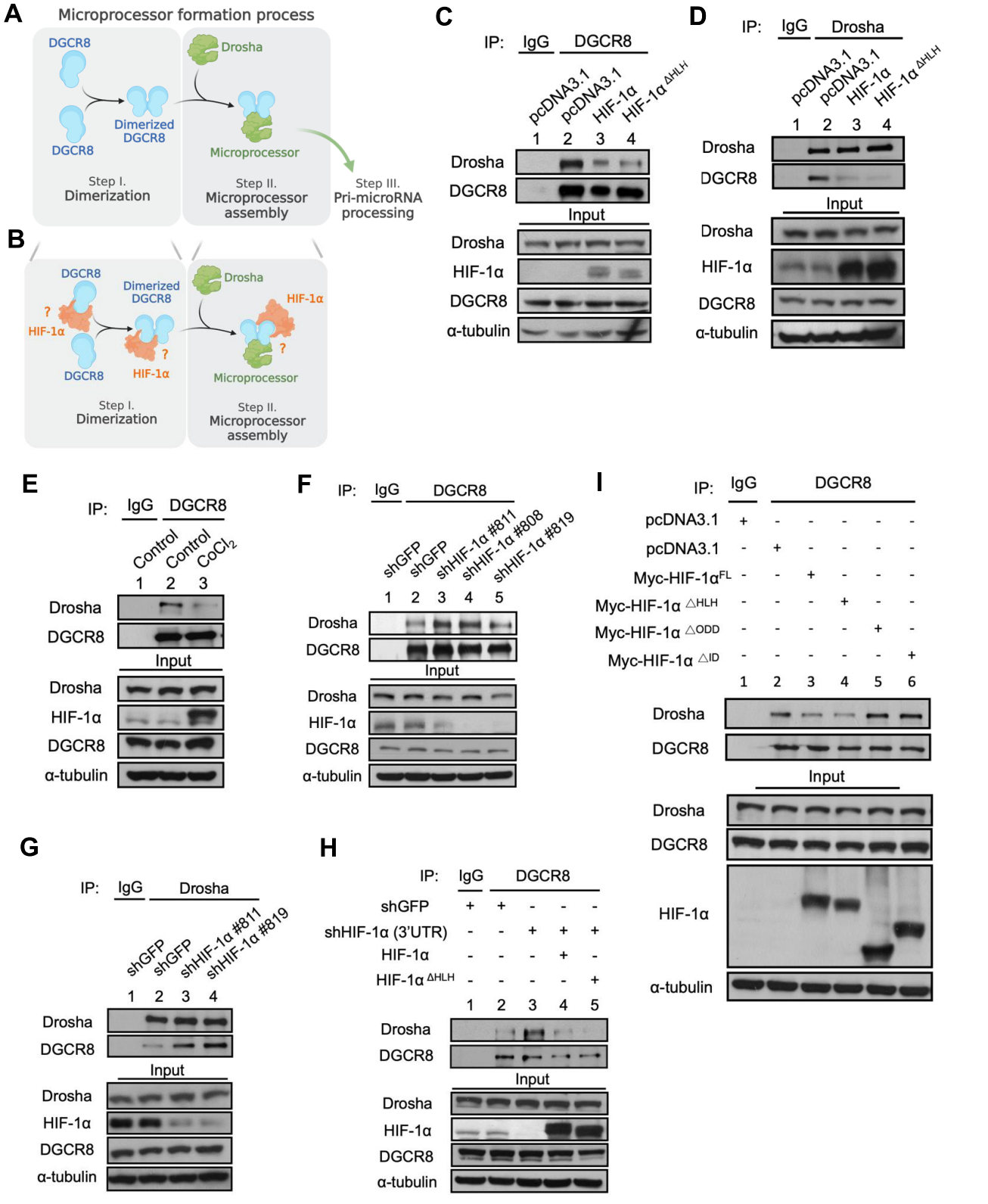

Figure 5. HIF-1α suppresses microprocessor formation. (**A**) Schematic representation of microprocessor formation process. (**B**) Possible mechanism of HIF-1α-suppressed microprocessor activity. (C–I) Microprocessor formation regulated by HIF-1α. Endogenous interaction between DGCR8 and Drosha in HIF-1α-expressing (**C, D**), HIF-1α- stabilized (**E**) and HIF-1α knockdown (**F, G**) HEK293T cells. (**H**) Endogenous binding of DGCR8 with Drosha in HIF-1α knockdown HEK293T cells with restoration of wild-type HIF-1α or HIF-1α$^{\Delta HLH}$. (**I**) Effects of truncated HIF-1α on microprocessor formation. Microprocessor formation was detected by immunoprecipitating either DGCR8 (C, E, F, H, I) or Drosha (D and G).

were conducted in a transcription-independent manner as the HLH-truncated HIF-1α also showed similar inhibitory effects on the microprocessor level (Figure 5C and D, lane 4), which were further confirmed by restoring either wild-type or HLH-truncated HIF-1α in knockdown cells (Figure 5H, lanes 4–5). As the ODD and ID domains of HIF-1α protein are essential for DGCR8 binding (Figure 4B), the restored microprocessor complexes were observed in cells expressing both truncation forms of HIF-1α (Figure 5I, lanes 5–6). There are two essential steps sequentially happening during microprocessor formation, which include the initial dimerization of DGCR8 and microprocessor formation with Drosha (Figure 5A). Thus, we further dissected the involvement of HIF-1α in DGCR8 dimerization (Figure 5B). First, we co-expressed DGCR8 with two different tags, and found that decreased V5-DGCR8 interaction with Flag-DGCR8 is detected in cells ectopically expressed HIF-1α (Figure 6A). The results suggested that HIF-1α inhibits dimerization of DGCR8, which was also supported by further experiments utilizing two DGCR8 mutants containing point mutations on tryptophan 329 essential for DGCR8 dimerization (DGCR8^{W329A} and DGCR8^{W329H}) (32,43,44). As expected, DGCR8^{W329A}/^{W329H} losing its dimerization ability showed reduced microprocessor formation; while interestingly, the enhanced affinity of monomeric DGCR8 with HIF-1α suggested a suppressive effect of HIF-1α on DGCR8 dimerization (Figure 6B). In addition, we performed *in vitro* processing assays using extracts from knockdown cells lacking HIF-1α, or extracts from cells with ectopic expression of either wild-type or HLH-truncated HIF-1α. *In vitro* transcription producing different primary transcripts of miRNAs (pri-let-7a, pri-let-7b, pri-let-7d, pri-let-7e, pri-let-7g, pri-miR-16-1, pri-miR-29a, pri-miR-29b and pri-miR-205) was conducted to prepare a panel of unprocessed subtracts for microprocessor. We found a significant accumulation among all of the unprocessed pri-miRNAs and reduced pre-miRNAs in cells expressing HIF-1α, while similar effects were also observed in cells expressing HLH-truncated HIF-1α (Figure 6C, D). In contrast, these unprocessed pri-miRNAs and pre-miRNAs were reduced and accumulated, respectively, in cells lacking HIF-1α (Figure 6E–H). These findings indicated that HIF-1α not only interacts with DGCR8, but also prevents DGCR8 dimerization prior to the complete microprocessor formation, leading to suppressed miRNAs nuclear processing.

Biological involvement of HIF-1α in regulating microprocessor function

Having confirmed that HIF-1α interacts with DGCR8 to suppress microprocessor formation, we further investigated whether this mechanism is also functionally controlled under biological stimulations as well as in model organisms. First, we found the reduced microprocessor formation under hypoxia and EGF treatment along with HIF-1α stimulation (Figure 7A, lanes 2 versus 3; Figure 7B, lanes 1 versus 2). Furthermore, we combined HIF-1α knockdown under either hypoxia or EGF treatment and observed a significant restoration of the microprocessor complex (Figure 7A, lanes 2 versus 4; Figure 7B, lanes 3 versus 5), which confirmed the involvement of HIF-1α in the suppression of microprocessor formation under these biological stimulations. Furthermore, the reciprocal molecular conversion has existed in *C. elegans* with either gain- or loss-of-function of HIF-1 (Supplementary Figure S2A, B), in which the reduced PASH-1/DRSH-1 complex was observed in sustainedly-expressed hif-1 strain (*ials34*), whereas the facilitated PASH-1/DRSH-1 assembly was observed in deletion mutant *hif-1* strain (*ia4*) (Figure 7C, D). Since it is well known that HIF-1α is biologically induced in human cancer (45,46), we simultaneously determined the existence of DGCR8/HIF-1α and Drosha/DGCR8 by performing PLA detection using human breast cancer tissues (Figure 7E), and observed a dramatically reduced pattern of microprocessor complex (Figure 7E, F, Drosha/DGCR8; green) in tissues with higher expression of HIF-1α #D10 and #E2 (upper two panels) compared with lower expression of HIF-1α #11 and #27 (lower two panels) along with more DGCR8 interaction with HIF-1α (Figure 7E-F, DGCR8/HIF-1α; yellow), while the statistical analyses also showed significant inversed correlation ($r = -0.49$, $P < 0.0001$). Also, a widespread reduction of miRNAs over 50% in tumors with higher HIF-1α expression was consistently observed among multiple human malignancies (Figure 7G). As a functional consequence, the unprocessed pri-miRNAs were accumulated under hypoxia and EGF-treated cells (Figure 7H, I, lane 2), while again, knockdown of HIF-1α mitigated these biologically-induced accumulations of microprocessor substrates (Figure 7H, I, lane 3). Taken together, our results demonstrated that HIF-1α binds to monomeric DGCR8 to suppress their dimerization and subsequently results in impaired microprocessor formation at the initial assembling phase, eventually leading to suppressed processing of pri-miRNAs.

Discussion

As the first essential step for miRNA maturation, the regulatory mechanisms that modulate microprocessor activity, especially targeting Drosha, have been studied by previous reports (17). At the transcriptional level, the *DROSHA* gene is transactivated by c-Myc to facilitate miRNA biogenesis (47). Also, several auxiliary factors such as BRCA1, P53, transforming growth factor beta (TGF-β), bone morphogenetic protein (BMP), and KH-type splicing regulatory protein (KSRP) have been reported to physically interact with Drosha for promoting miRNA maturation (48–53). On the other hand, the nuclear YAP sequesters p72 (DDX17) for suppressing microprocessor function at low cell density (30). MTOR-mediated proteasomal degradation of Drosha by activation of E3 ligases, MDM2, also results in downregulated miRNA maturation (54). In this study, we unveiled the molecular mechanism that instead of directly targeting Drosha, HIF-1α protein physically interacts with monomeric DGCR8 therefore preventing its dimerization, leading to suppressed microprocessor formation and reduced primary miRNA precursor cleavage. This finding provided new evidence of how microprocessor activity could be biologically controlled at the initial step of complex assembly.

HIF-1α is a stress-sensitive protein activated to undergo certain stimulations, thereby utilizing its canonical transcriptional activity for cellular adaption (25); however, only limited studies reported the non-canonical function of HIF-1α. Villa *et al*. found that HIF-1α binds and activates γ-secretase [48]. Hubbi *et al*. observed that HIF-1α interacts with CDC6 through the N-terminal domain and promotes the interaction between CDC6 and MCM complex (55). As a molecular hub for sensing microenvironmental changes, we demonstrated that the induction of HIF-1α by either hypoxia or

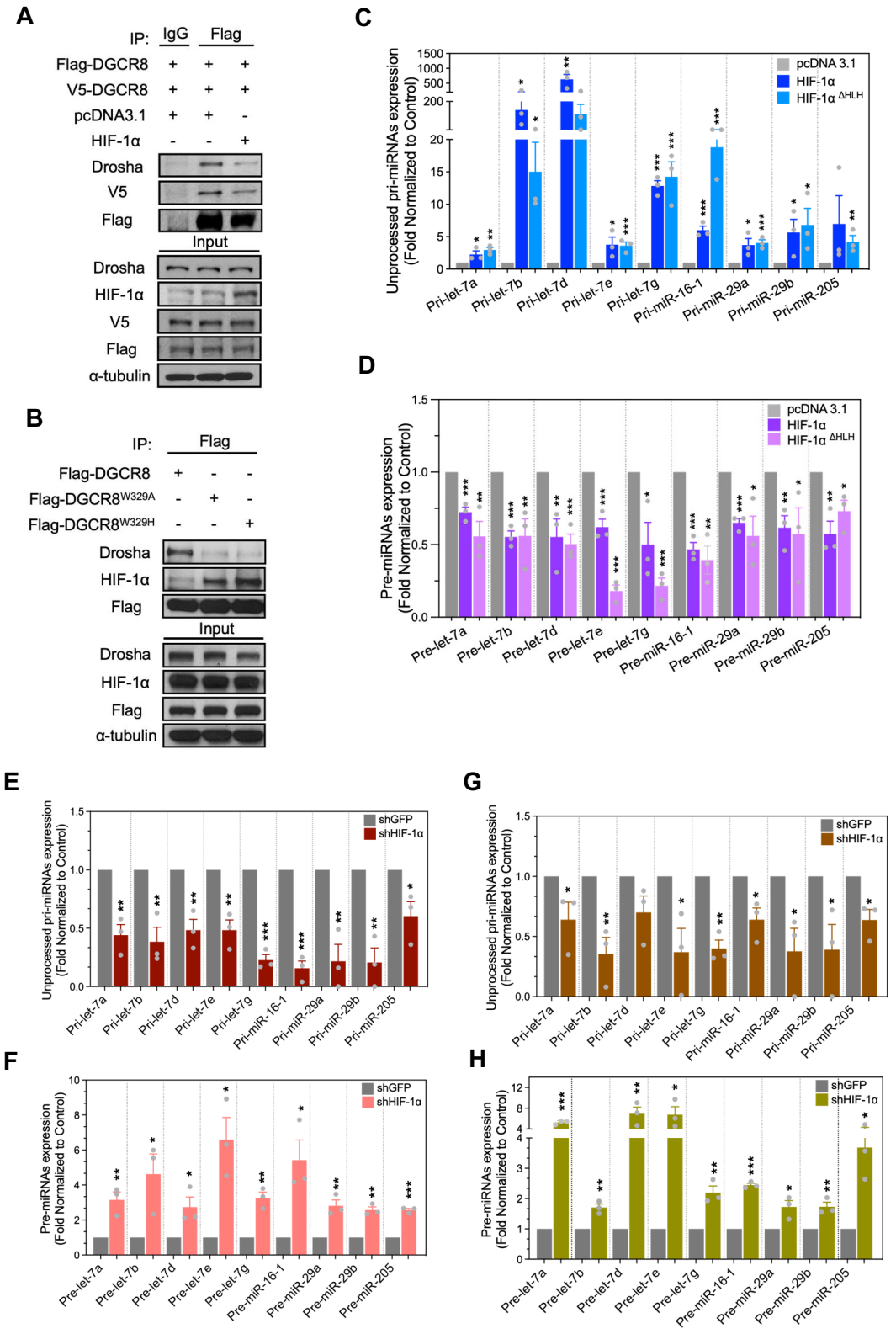

Figure 6. HIF-1α abolishes DGCR8 dimerization to reduce microprocessor formation and processing ability. (**A**) Dimerization level of DGCR8 was determined by co-expression of Flag- and V5-tagged DGCR8 following immunoprecipitation of Flag tag. (**B**) Interaction of HIF-1α with monomeric DGCR8. Monomeric DGCR8 (Flag-DGCR8^{W329A} and Flag-DGCR8^{W329H}) were immunoprecipitated for determining HIF-1α binding. (**C–H**) *In vitro* processing assays of unprocessed pri-miRNAs. Unprocessed pri-miRNAs generated from *in vitro* transcription were incubated with extracts expressing either wild-type or HLH-truncated HIF-1α (C, D, HEK293T cells) or lacking HIF-1α (E, F, MDA-MB-231 cells; G, H, MCF-7 cells) for 30 min at 37°C in *in vitro* processing buffer. Detection of unprocessed pri-miRNAs (**C**, **E**, **G**) or pre-miRNAs (**D**, **F**, **H**) after *in vitro* processing assay. Data were represented as mean ± SEM ($n \geq 3$) with individual data point shown. $^{*}P < 0.05$, $^{**}P < 0.01$, $^{***}P < 0.001$.

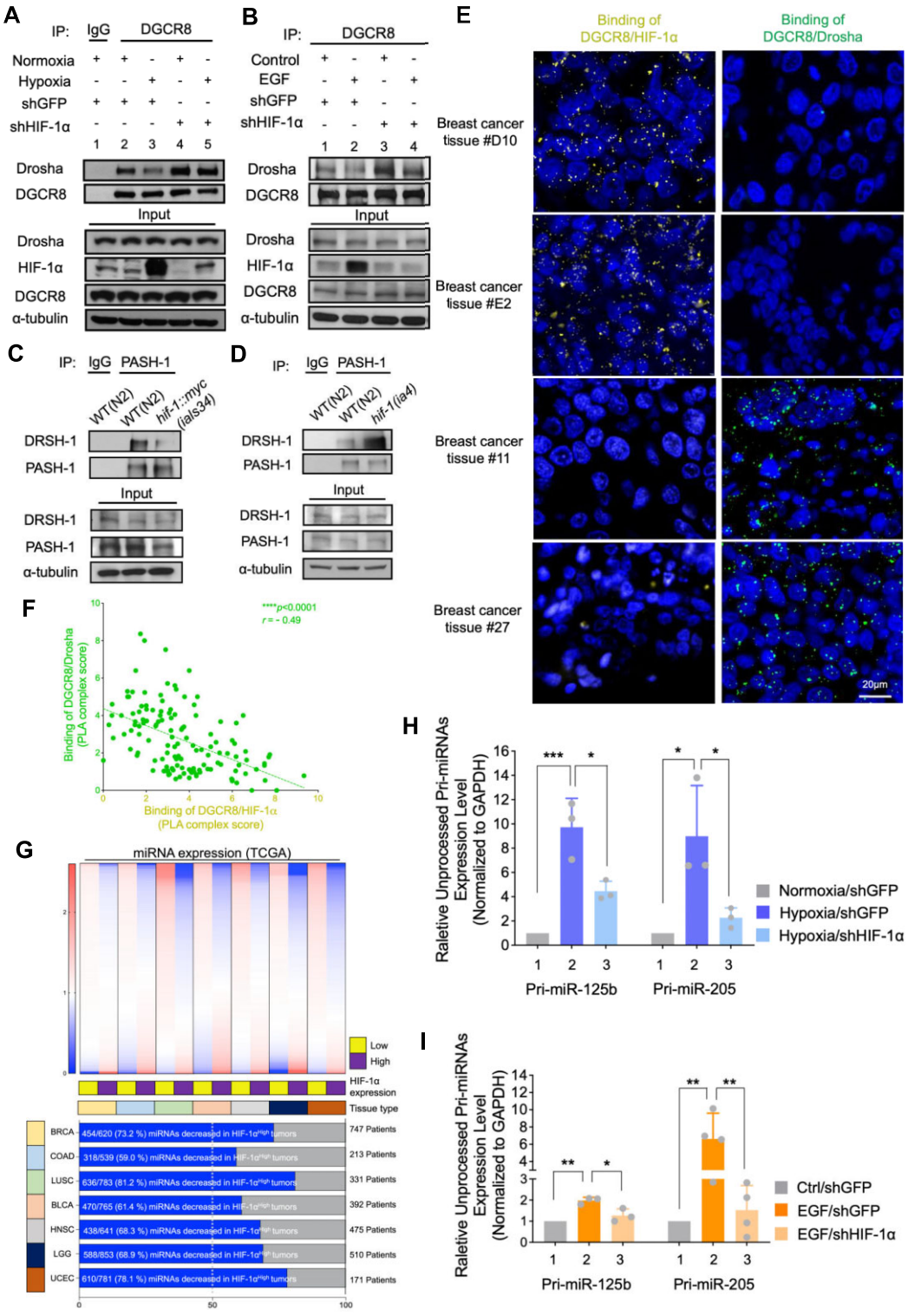

Figure 7. Biological impacts of HIF-1α on suppressing microprocessor assembly and function. (**A**, **B**) Microprocessor formation regulated by HIF-1α-inducing stresses. Interaction of DGCR8/Drosha in hypoxic (A, MCF7 cells) or EGF-treated (B, MDA-MB-231 cells) HIF-1α knockdown cells. (**C, D**) Microprocessor formation regulated by HIF-1α in *C.elegans*. Interaction between DRSH-1 and PASH-1 in wild type (N2), *ials34* (sustainedly-expressed *hif-1* strain, C) and *ia4* (deletion mutant *hif-1* strain, D) *C.elegans* strains (59,60). (**E**) *In situ* bindings between DGCR8 and HIF-1α (yellow), DGCR8 and Drosha (green) were determined by PLA using human breast cancer tissue. Patient #D10 and #E2 was representative tissues with HIF-1α high expression and patient #11 and #27 were those with HIF- 1α low expression. (**F**) Correlation between binding of HIF-1α/DGCR8 and Drosha/DGCR8, analyzed by PLA complex score. (**G**) Global expression patterns of miRNA in human cancer tissues. Level of miRNAs in human cancer tissues (TCGA database) with corresponded to high/low HIF-1α expression. Data were divided into low/high group by mean value of HIF-1α. Upper panel showed the heatmap of individual miRNAs expression patterns in HIF-1α low or HIF- 1α high tumors from multiple cancer types. Bottom panel summarized the percentage of downregulated miRNAs in patients with higher HIF-1α expression in multiple cancer types. (H, I) Expression of unprocessed pri-miRNAs under HIF-1α-inducing stresses. Pri-miRNAs expression in hypoxic (**H**) or EGF-treated (**I**) HIF-1α knockdown cells. Data were represented as mean ± SEM ($n \geq 3$) with individual data point shown. $^{*}P < 0.05$, $^{**}P < 0.01$, $^{***}P < 0.001$.

growth factors is able to abolish microprocessor formation as well as its activity in a transcription-independent manner (Figures 3 and 7), this HIF-1α-inhibited microprocessor formation was also observed in human, *D. melanogaster*, and *C. elegans* (Figure 7), which demonstrated that HIF-1α orchestrates a highly conserved regulation to modulate microprocessor activity. Conversely, it is also possible that certain miRNAs, acting as feedback regulators, could regulate HIF-1α. Chiang *et al.* reported that miR-182 targets and downregulates several HIF-1α-destabilizing factors (PHD2, FIH1 and FBXW7), therefore miR-182 could serve as an upstream to indirectly enhance HIF-1α expression (56,57).

As two evolutionary conserved proteins, ODD and ID domains from HIF-1α and an uncharacterized region of amino acid 685–750 from DGCR8 were found to be essential for their interaction (Figure 4). From structure insight, protein region covering ODD and ID domains of HIF-1α are intrinsically disordered region (IDR) that is flexible for protein-protein interaction; on the other hand, the predicted HIF-1α-interacting region of DGCR8 appeared as a helical arch structure with relatively higher amino acid sequence homology observed in human, mouse, *D. melanogaster*, and *C. elegans* (Figure 4), while this HIF-1α-interacting region of DGCR8 also covered the known Drosha-binding elements (Figure 4), leading us to proposed the inhibitory effect of HIF-1α on microprocessor assembly. Detailly, HIF-1α was later found to interfere microprocessor formation through binding to DGCR8, as higher affinity of HIF-1α with monomeric DGCR8 prevented Drosha binding at the initial step of microprocessor assembly (Figures 5 and 6).

Data availability

All data are available in the main text or the supplementary materials.

Supplementary data

Supplementary Data are available at NAR Online.

Acknowledgements

We are grateful to Dr Chien-Hung Yu and Dr Shaw-Jenq Tsai for involving conceptualization during manuscript preparation. We thank Dr Hsueh-Cheng Chiang for animal experiments support. We thank Dr Chyuan-Chuan Wu for protein structure simulation support. We thank Dr Richard I. Gregory, V. Narry Kim, and Feng Guo. for sharing their plasmids. We thank Dr Chih-Chen Hong for technical support. We are grateful for the support from the Human Biobank, Research Center of Clinical Medicine, and the Cancer Data Bank of the Cancer Center, National Cheng Kung University Hospital. We thank the technical services provided by the 'Bioimage Core Facility of the National Core Facility Program for Biotechnology, National Science and Technology Council, Taiwan'. We thank the National RNAi Core Facility at Academia Sinica in Taiwan for providing shRNA reagents and related services. We thank the staff of the Biomedical Resource Core at the First Core Labs, National Taiwan University College of Medicine, for technical assistance. This study was supported by the Ministry of Science and Technology, Taiwan (Excellent Young Scholar Grant; PSC; MOST 103-2628-B-006–003-MY3); by the Ministry of Science and Technology, Taiwan (2030 Cross-Generation Young Scholars Program - Excellent Young Scholar Grant; PSC; MOST 111–2628-B-006–014-MY3); by the Ministry of Science and Technology, Taiwan (PSC; 108-2320-B-006–041-MY3); by the Ministry of Science and Technology, Taiwan (PSC; 107-2320-B-006-068); by the Ministry of Science and Technology, Taiwan (PSC; 106-2320-B-006-038); by National Science and Technology Council, Taiwan (Ta-You Wu Memorial Award Grant, 112-2326-B-006-001-MY3). The graphical abstract and schematic representations in the figures were created using Biorender.com.

Author contributions: Conceptualization: J.N.L., P.S.C.; Methodology: J.N.L., P.S.C., M.S.C., Y.J.L., P.B., M.S.C., Y.H.W; Investigation: J.N.L., P.S.C., M.Y.W., Y.J.L., Y.H.W; Visualization: J.N.L.; Funding acquisition: P.S.C.; Project administration: J.N.L., P.S.C., M.Y.W., J.W.R; Supervision: P.S.C.; Writing-original draft: J.N.L., P.S.C.; Writing-review & editing: J.N.L., P.S.C., M.Y.W.

Funding

Ministry of Science and Technology, Taiwan [Excellent Young Scholar Grant; PSC; MOST 103-2628-B-006-003-MY3]; Ministry of Science and Technology, Taiwan [2030 Cross-Generation Young Scholars Program - Excellent Young Scholar Grant; PSC; MOST 111-2628-B-006-014-MY3]; Ministry of Science and Technology, Taiwan [PSC; 108-2320-B-006-041-MY3]; Ministry of Science and Technology, Taiwan [PSC; 107-2320-B-006-068]; Ministry of Science and Technology, Taiwan [PSC; 106-2320-B-006-038]; National Science and Technology Council, Taiwan [Ta-You Wu Memorial Award Grant, 112-2326-B-006-001-MY3]. Funding for open access charge: National Science and Technology Council, Taiwan [Ta-You Wu Memorial Award Grant, 112-2326-B-006-001-MY3].

Conflict of interest statement

None declared.

References

1. Lin,S.B. and Gregory,R.I. (2015) MicroRNA biogenesis pathways in cancer. *Nat. Rev. Cancer*, **15**, 321–333.
2. Winter,J., Jung,S., Keller,S., Gregory,R.I. and Diederichs,S. (2009) Many roads to maturity: microRNA biogenesis pathways and their regulation. *Nat. Cell Biol.*, **11**, 228–234.
3. Shang,R.F., Lee,S., Senavirathne,G. and Lai,E.C. (2023) microRNAs in action: biogenesis, function and regulation. *Nat. Rev. Genet.*, **24**, 816–833.
4. Ha,M. and Kim,V.N. (2014) Regulation of microRNA biogenesis. *Nat. Rev. Mol. Cell Biol.*, **15**, 509–524.
5. Rana,T.M. (2007) Illuminating the silence: understanding the structure and function of small RNAs. *Nat. Rev. Mol. Cell Biol.*, **8**, 23–36.
6. Dalmay,T. (2008) MicroRNAs and cancer. *J. Intern. Med.*, **263**, 366–375.
7. Jakymiw,A., Pauley,K.M., Li,S.Q., Ikeda,K., Lian,S.L., Eystathioy,T., Satoh,M., Fritzler,M.J. and Chan,E.K.L. (2007) The role of GW/P-bodies in RNA processing and silencing. *J. Cell Sci.*, **120**, 1317–1323.
8. Lee,O. and Kim,V.N. (2004) Evidence that microRNA genes are transcribed by RNA polymerase II. *Cell Struct. Funct.*, **29**, 68–68.
9. Lee,Y., Ahn,C., Han,J.J., Choi,H., Kim,J., Yim,J., Lee,J., Provost,P., Radmark,O., Kim,S., *et al.* (2003) The nuclear RNase III Drosha initiates microRNA processing. *Nature*, **425**, 415–419.

10. Zhang,H.D., Kolb,F.A., Jaskiewicz,L., Westhof,E. and Filipowicz,W. (2004) Single processing center models for human dicer and bacterial RNase III. *Cell*, **118**, 57–68.
11. MacRae,I.J., Zhou,K.H., Li,F., Repic,A., Brooks,A.N., Cande,W.Z., Adams,P.D. and Doudna,J.A. (2006) Structural basis for double-stranded RNA processing by dicer. *Science*, **311**, 195–198.
12. Filippov,V., Solovyev,V., Filippova,M. and Gill,S.S. (2000) A novel type of RNase III family proteins in eukaryotes. *Gene*, **245**, 213–221.
13. Gregory,R.I., Yan,K.P., Amuthan,G., Chendrimada,T., Doratotaj,B., Cooch,N. and Shiekhattar,R. (2004) The Microprocessor complex mediates the genesis of microRNAs. *Nature*, **432**, 235–240.
14. Yeom,K.H., Lee,Y., Han,J., Suh,M.R. and Kim,V.N. (2006) Characterization of DGCR8/Pasha, the essential cofactor for Drosha in primary miRNA processing. *Nucleic Acids Res.*, **34**, 4622–4629.
15. Zeng,Y., Yi,R. and Cullen,B.R. (2005) Recognition and cleavage of primary microRNA precursors by the nuclear processing enzyme Drosha. *EMBO J.*, **24**, 138–148.
16. Nguyen,T.A., Jo,M.H., Choi,Y.G., Park,J., Kwon,S.C., Hohng,S., Kim,V.N. and Woo,J.S. (2015) Functional anatomy of the human microprocessor. *Cell*, **161**, 1374–1387.
17. Treiber,T., Treiber,N. and Meister,G. (2019) Regulation of microRNA biogenesis and its crosstalk with other cellular pathways. *Nat. Rev. Mol. Cell Biol.*, **20**, 5–20.
18. Kuschel,A., Simon,P. and Tug,S. (2012) Functional regulation of HIF-1alpha under normoxia–is there more than post-translational regulation? *J. Cell. Physiol.*, **227**, 514–524.
19. Cimmino,F., Avitabile,M., Lasorsa,V.A., Montella,A., Pezone,L., Cantalupo,S., Visconte,F., Corrias,M.V., Iolascon,A. and Capasso,M. (2019) HIF-1 transcription activity: HIF1A driven response in normoxia and in hypoxia. *BMC Med. Genet.*, **20**, 37.
20. Zhong,H., Chiles,K., Feldser,D., Laughner,E., Hanrahan,C., Georgescu,M.M., Simons,J.W. and Semenza,G.L. (2000) Modulation of hypoxia-inducible factor 1 alpha expression by the epidermal growth factor/phosphatidylinositol 3-kinase/PTEN/AKT/FRAP pathway in human prostate cancer cells: Implications for tumor angiogenesis and therapeutics. *Cancer Res.*, **60**, 1541–1545.
21. Piret,J.P., Lecocq,C., Toffoli,S., Ninane,N., Raes,M. and Michiels,C. (2004) Hypoxia and CoCl2 protect HepG2 cells against serum deprivation- and t-BHP-induced apoptosis: a possible anti-apoptotic role for HIF-1. *Exp. Cell Res.*, **295**, 340–349.
22. Thomas,R. and Kim,M.H. (2008) HIF-1 alpha: a key survival factor for serum-deprived prostate cancer cells. *Prostate*, **68**, 1405–1415.
23. Bonello,S., Zahringer,C., BelAiba,R.S., Djordjevic,T., Hess,J., Michiels,C., Kietzmann,T. and Gorlach,A. (2007) Reactive oxygen species activate the HIF-1 alpha promoter via a functional NF kappa B site. *Arterioscler. Thromb. Vasc. Biol.*, **27**, 755–761.
24. Cho,K.H., Choi,M.J., Jeong,K.J., Kim,J.J., Hwang,M.H., Shin,S.C., Park,C.G. and Lee,H.Y. (2014) A ROS/STAT3/HIF-1alpha signaling cascade mediates EGF-induced TWIST1 expression and prostate cancer cell invasion. *Prostate*, **74**, 528–536.
25. Koh,M.Y., Spivak-Kroizman,T.R. and Powis,G. (2008) HIF-1 regulation: not so easy come, easy go. *Trends Biochem. Sci.*, **33**, 526–534.
26. Lai,H.H., Li,J.N., Wang,M.Y., Huang,H.Y., Croce,C.M., Sun,H.L., Lyu,Y.J., Kang,J.W., Chiu,C.F., Hung,M.C., *et al.* (2018) HIF-1 alpha promotes autophagic proteolysis of Dicer and enhances tumor metastasis. *J. Clin. Invest.*, **128**, 625–643.
27. Bustin,S.A., Benes,V., Garson,J.A., Hellemans,J., Huggett,J., Kubista,M., Mueller,R., Nolan,T., Pfaffl,M.W., Shipley,G.L., *et al.* (2009) The MIQE Guidelines: minimum information for publication of quantitative real-time PCR experiments. *Clin. Chem.*, **55**, 611–622.
28. Yin,S.Y., Yu,Y. and Reed,R. (2015) Primary microRNA processing is functionally coupled to RNAP II transcription. *Sci. Rep.*, **5**, 11992.
29. Fernandez,N., Cordiner,R.A., Young,R.S., Hug,N., Macias,S. and Cáceres,J.F. (2017) Genetic variation and RNA structure regulate microRNA biogenesis. *Nat. Commun.*, **8**, 15114.
30. Mori,M., Triboulet,R., Mohseni,M., Schlegelmilch,K., Shrestha,K., Camargo,F.D. and Gregory,R.I. (2014) Hippo signaling regulates microprocessor and links cell-density-dependent miRNA biogenesis to cancer. *Cell*, **156**, 893–906.
31. Han,J., Pedersen,J.S., Kwon,S.C., Belair,C.D., Kim,Y.K., Yeom,K.H., Yang,W.Y., Haussler,D., Blelloch,R. and Kim,V.N. (2009) Posttranscriptional crossregulation between Drosha and DGCR8. *Cell*, **136**, 75–84.
32. Senturia,R., Faller,M., Yin,S., Loo,J.A., Cascio,D., Sawaya,M.R., Hwang,D., Clubb,R.T. and Guo,F. (2010) Structure of the dimerization domain of DiGeorge critical region 8. *Protein Sci.*, **19**, 1354–1365.
33. Heo,I., Joo,C., Cho,J., Ha,M., Han,J.J. and Kim,V.N. (2008) Lin28 mediates the terminal uridylation of let-7 precursor microRNA. *Mol. Cell*, **32**, 276–284.
34. Chiang,H.R., Schoenfeld,L.W., Ruby,J.G., Auyeung,V.C., Spies,N., Baek,D., Johnston,W.K., Russ,C., Luo,S.J., Babiarz,J.E., *et al.* (2010) Mammalian microRNAs: experimental evaluation of novel and previously annotated genes. *Gene Dev.*, **24**, 992–1009.
35. Kim,J.W., Tchernyshyov,I., Semenza,G.L. and Dang,C.V. (2006) HIF-1-mediated expression of pyruvate dehydrogenase kinase: a metabolic switch required for cellular adaptation to hypoxia. *Cell Metab.*, **3**, 177–185.
36. Weber-Boyvat,M., Li,S., Skarp,K.P., Olkkonen,V.M., Yan,D. and Jantti,J. (2015) Bimolecular fluorescence complementation (BiFC) technique in yeast Saccharomyces cerevisiae and mammalian cells. *Methods Mol. Biol.*, **1270**, 277–288.
37. Harmon,M., Larkman,P., Hardingham,G., Jackson,M. and Skehel,P. (2017) A Bi-fluorescence complementation system to detect associations between the endoplasmic reticulum and mitochondria. *Sci. Rep.*, **7**, 17467.
38. Becker,S. and von Einem,J. (2013) Detection of protein interactions during virus infection by bimolecular fluorescence complementation. *Methods Mol. Biol.*, **1064**, 29–41.
39. Bondos,S.E., Dunker,A.K. and Uversky,V.N. (2021) On the roles of intrinsically disordered proteins and regions in cell communication and signaling. *Cell Commun. Signal.*, **19**, 88.
40. Pierce,B.G., Wiehe,K., Hwang,H., Kim,B.H., Vreven,T. and Weng,Z.P. (2014) ZDOCK server: interactive docking prediction of protein-protein complexes and symmetric multimers. *Bioinformatics*, **30**, 1771–1773.
41. Schneidman-Duhovny,D., Inbar,Y., Nussinov,R. and Wolfson,H.J. (2005) PatchDock and SymmDock: servers for rigid and symmetric docking. *Nucleic Acids Res.*, **33**, W363–W367.
42. Laskowski,R.A., Jablonska,J., Pravda,L., Varekova,R.S. and Thornton,J.M. (2018) PDBsum: Structural summaries of PDB entries. *Protein Sci.*, **27**, 129–134.
43. Weitz,S.H., Gong,M., Barr,I., Weiss,S. and Guo,F. (2014) Processing of microRNA primary transcripts requires heme in mammalian cells. *P. Natl. Acad. Sci. U.S.A.*, **111**, 1861–1866.
44. Senturia,R., Laganowsky,A., Barr,I., Scheidemantle,B.D. and Guo,F. (2012) Dimerization and heme binding are conserved in amphibian and starfish homologues of the microRNA processing protein DGCR8. *PLoS One*, **7**, e39688.
45. Soni,S. and Padwad,Y.S. (2017) HIF-1 in cancer therapy: two decade long story of a transcription factor. *Acta Oncol.*, **56**, 503–515.
46. Pezzuto,A. and Carico,E. (2018) Role of HIF-1 in cancer progression: novel insights. A review. *Curr. Mol. Med.*, **18**, 343–351.
47. Wang,X.W., Zhao,X.C., Gao,P. and Wu,M. (2013) c-Myc modulates microRNA processing via the transcriptional regulation of Drosha. *Sci. Rep.*, **3**, 01942.
48. Kawai,S. and Amano,A. (2012) BRCA1 regulates microRNA biogenesis via the DROSHA microprocessor complex. *J. Cell Biol.*, **197**, 201–208.

49. Suzuki,H.I., Yamagata,K., Sugimoto,K., Iwamoto,T., Kato,S. and Miyazono,K. (2009) Modulation of microRNA processing by p53. *Nature*, **460**, 529–533.
50. Davis,B.N., Hilyard,A.C., Lagna,G. and Hata,A. (2008) SMAD proteins control DROSHA-mediated microRNA maturation. *Nature*, **454**, 56–61.
51. Davis,B.N., Hilyard,A.C., Nguyen,P.H., Lagna,G. and Hata,A. (2010) Smad proteins bind a conserved RNA sequence to promote microRNA maturation by Drosha. *Mol. Cell*, **39**, 373–384.
52. Trabucchi,M., Briata,P., Garcia-Mayoral,M., Haase,A.D., Filipowicz,W., Ramos,A., Gherzi,R. and Rosenfeld,M.G. (2009) The RNA-binding protein KSRP promotes the biogenesis of a subset of microRNAs. *Nature*, **459**, 1010–1014.
53. Trabucchi,M., Briata,P., Filipowicz,W., Ramos,A., Gherzi,R. and Rosenfeld,M.G. (2010) KSRP promotes the maturation of a group of miRNA precursors. *Regul. MicroRNAs*, **700**, 36–42.
54. Ye,P.Y., Liu,Y., Chen,C., Tang,F., Wu,Q., Wang,X., Liu,C.G., Liu,X.P., Liu,R.H., Liu,Y., *et al.* (2015) An mTORC1-Mdm2-Drosha axis for miRNA biogenesis in response to glucose- and amino acid-deprivation. *Mol. Cell*, **57**, 708–720.
55. Hubbi,M.E., Kshitiz,Gilkes, D.M., Rey,S., Wong,C.C., Luo,W.B., Kim,D.H., Dang,C.V., Levchenko,A. and Semenza,G.L. (2013) A nontranscriptional role for HIF-1α as a direct inhibitor of DNA replication. *Sci. Signal*, **6**, ra10.
56. Chiang,C.H., Chu,P.Y., Hou,M.F. and Hung,W.C. (2016) MiR-182 promotes proliferation and invasion and elevates the HIF-1α-VEGF-A axis in breast cancer cells by targeting FBXW7. *Am. J. Cancer Res.*, **6**, 1785–1798.
57. Li,Y., Zhang,D., Wang,X.Y., Yao,X., Ye,C., Zhang,S.J., Wang,H., Chang,C.J., Xia,H.F., Wang,Y.C., *et al.* (2015) Hypoxia-inducible miR-182 enhances HIF1α signaling via targeting PHD2 and FIH1 in prostate cancer. *Sci. Rep.*, **5**, 12495.
58. Jumper,J., Evans,R., Pritzel,A., Green,T., Figurnov,M., Ronneberger,O., Tunyasuvunakool,K., Bates,R., Zidek,A., Potapenko,A., *et al.* (2021) Highly accurate protein structure prediction with AlphaFold. *Nature*, **596**, 583–589.
59. Zhang,Y., Shao,Z.Y., Zhai,Z.W., Shen,C. and Powell-Coffman,J.A. (2009) The HIF-1 hypoxia-inducible factor modulates lifespan in *C. elegans*. *PLoS One*, **4**, e6348.
60. Jiang,H.Q., Guo,R. and Powell-Coffman,J.A. (2001) The hif-1 gene encodes a bHLH-PAS protein that is required for adaptation to hypoxia. *Proc. Natl. Acad. Sci. U.S.A.*, **98**, 7916–7921.

Received: January 5, 2024. **Revised:** August 22, 2024. **Editorial Decision:** August 27, 2024. **Accepted:** August 31, 2024